Supporting Information

Materials and Methods

Cell culture

HCT116, p53KO, p21KO, and p21/PUMA DKO cells were a kind gift of Bert Vogelstein (Johns Hopkins Medical School). RKO, ACHN, LOX IMVI, UACC62, CAKI, NCI H460, DLD1, SW480, A375.S2 and U2OS cells were obtained from National Cancer Institute as part of the NCI 60 panel of cancer cell lines and from American Type Culture Collection (ATCC). The *p21* expression vector was a kind gift of William G. Kaelin (Dana Farber Cancer Institute). Cell lines were grown as recommended. *TERT* shRNAs were a kind gift of William Hahn (Harvard University). Lentiviral shRNA expression vectors were obtained from OpenBiosystems and were packaged by co-transfecting with lentiviral packaging plasmids into 293T cells using Effectene (Qiagen). After infection with lentivirus shRNA particles, cells stably transduced with lentiviral DNA were selected in medium containing puromycin. Cells were treated with 2.5 μM imetelstat or mismatch oligonucleotides (Geron Corporation) twice per week for up to 6 weeks and did not exceed 80% confluence during the treatment. Cells were treated with indicated concentrations of UC2288 at 80% confluence during the treatment. Cells were treated with indicated concentrations of CP-31398 at 80% confluence during the treatment.

Cell viability and colony formation assay

For viability assays, cells were mixed with an equal volume of Trypan Blue Solution (Invitrogen) and counted using Countess (Invitrogen). For colony formation assays, 10^3 cells were seeded in triplicate. Colonies were stained with 0.005% crystal-violet solution and counted after 10 days.

Nanoparticle Synthesis

PLGA nanoparticles loaded with siRNA were fabricated using a double emulsion solvent evaporation method and coated with ANTP as previously described (37). After washing unencapsulated siRNA and unattached ANTP, nanoparticles were lyophilized with the cryoprotectant, trehalose, at an equal mass ratio of polymer to carbohydrate.

Tumorigenesis assays

Eight-week old, athymic nude (NCr nu/nu) mice (n=5) were injected subcutaneously with cancer cells ($2.5x10^6$). After one week, tumor-bearing mice received mismatch oligonucleotide or imetelstat (30 mg/kg bodyweight) three times per week by intraperitoneal injection. Sorafenib was dissolved in Cremophor EL/95% ethanol (50:50) (Sigma) as a 4X stock solution and diluted with sterile water before use. Sorafenib (15 mg/kg) was administered by oral gavage three times per week. UC2888 was dissolved in Oleic acid with PEG400 as a 4X stock solution. UC2288 (15mg/kg body weight) was administered by oral gavage three times per week. For experiments using nanoparticles mice were injected with p21 or non-specific siRNA (1.0 mg/Kg body) two times a week. CP-31398 was administered at the concentration of 25 mg/kg everyday. Tumor growth was measured using calipers, and tumor volumes were calculated using the formula 0.5 X length X $width^2$. TUNEL assays were performed as described previously (1). For body weight measurements, mice were weighed at the end of the experiments before sacrifice. Blood was collected from the tail vein for alkaline aminotransferase (ALT), aspratate aminotransferase (AST) and alkaline phosophatase (AP) activity analysis. ALT, AST and AP activities were measured using kits from Sigma-Aldrich. For complete blood analyses we did the following

experiments: Hematocrit (Packed red cell volume) was analyzed and calculated as percentage of packed cell volume to the total volume. For RBC count 10 μl whole blood was diluted 1:1000 with PBS and RBC were counted using hemocytometer. For white blood cell count, we mixed 10 μl whole blood with RBC lysis reagent and after 1 minute of incubation the white cells were counted by hemocytometer. For measuring kidney function and as an indicator of glomerular filtration rate Serum creatinine levels were measured using Creatinine assay kit as per the manufacturers recommendations (Abcam).

Quantitative RT-PCR analysis

Total RNA was extracted with TRIzol (Invitrogen) and purified using RNAeasy mini columns (Qiagen). First-strand cDNA was generated using ProtoScript M-MuLV First-Strand cDNA Synthesis Kit (New England Biolabs), and quantitative PCR was performed using Power SYBR Green PCR Master Mix (Applied Biosystems). *p21*, *PUMA*, *BAX*, *BAK*, *TERT*, *MDC1, NBS1 CDKN1B (p27)* and *E2F1* expression were analyzed using primers listed in Table S3. *Actin* mRNA was measured as an internal control.

Immunoblot analysis

Cell lysates were prepared using Pierce IP Lysis Buffer (Thermo Scientific) containing Protease Inhibitor Cocktail (Roche) and Phosphatase Inhibitor Cocktail (Sigma-Aldrich, St. Louis, MO). Protein concentration was estimated using a Bradford Protein Assay kit (Bio-Rad Laboratories). Proteins were separated on 10% or 12% polyacrylamide gels and transferred to PVDF membranes using a Bio-Rad Trans-Blot wet transfer apparatus. Membranes were blocked with 5% nonfat milk and probed with primary antibodies followed by the appropriate secondary HRP-

conjugated antibody (GE healthcare, UK). Blots were developed using the SuperSignal West Pico Chemiluminescent Substrate (Pierce). Antibody information is provided in Table S3.

FACS and Annexin V-FITC staining

FACS analyses for sub G1 cell population were done as described previously (2). Briefly cells were fixed with 70% ethanol for overnight. The following day, cells were washed twice with 1X PBS and resuspended in 300 µl of 1X PBS, treated with RNAase (Sigma-Aldrich) and Propidium iodide for 1 hr and analyzed using FACSCaliber (BD Biosciences). Annexin V-FITC/PE staining were performed as described previously (3) using a kit available from BD Bioscience, stained cells were analyzed using FACSCaliber (BD Biosciences).

TRAP assay

The TRAP assay was performed essentially as described (4). Briefly, cells were washed once with ice cold PBS, resuspended in 100µL of ice-cold CHAPS lysis buffer (10 mM Tris-HCl (pH 7.5), 1 mM $MgCl_2$, 1 mM EGTA, 0.5% CHAPS, 10% glycerol and 5 mM beta-mercaptoethanol) and incubated 25 min on ice to lyse. Lysates were centrifuged for 20 min at 13,000 rpm at 4°C, supernatants were collected, and protein concentrations were measured using a Bradford Protein Assay Kit (Bio-Rad Laboratories). For the preparation of lysates equal weight tumor tissue was homogenized and processed similar to as described above. Telomerase activity was measured using a SYBR Green RQ-TRAP assay with 750 ng lysate, 0.1 µg telomerase primer TS and 0.05 µg anchored return primer ACX in a 25 µl reaction volume with SYBR Green PCR Master Mix (Applied Biosystems). TS and ACX primer sequences are provided in Table S3. Samples were analyzed using a CFX96 thermal cycler (Bio-Rad laboratories) by incubating for 20 minutes at

25°C, and amplified in a 35 cycle, two-step PCR with the conditions: 30 seconds at 95°C, and 90 seconds at 60°C. The threshold cycle values (Ct) were determined from semi-log amplification plots (log increase in fluorescence versus cycle number). Every plate included standards, inactivated samples and lysis buffer as controls. Each sample was analyzed at least in triplicate. Telomerase activity was plotted relative to untreated cells.

Telomere PNA FISH analysis

Peptide Nucleic Acid Fluorescence In Situ Hybridization (PNA FISH) was performed as described (5). Briefly, cells were treated with 0.5 μg/ml of colcemid for 3.5 hrs to arrest cells in metaphase. Trypsinized cells were incubated in 0.6 M KCl, fixed with methanol:acetic acid (3:1) and spread on glass slides. Metaphase chromosome spreads were hybridized with the telomeric PNA probe, 5′-Tam-OO-$(CCCTAA)_4$-3′. Chromosome images and telomere signals were captured and processed using a Nikon Eclipse 80i microscope and NIS-elements BR 3.1 software. At least 1000 chromosomes per sample were scored for telomere loss (i.e., signal free ends).

Terminal Restriction Fragment (TRF) analysis

Terminal Restriction Fragment (TRF) southern blot analysis was performed as described (6). Briefly, cells were trypsinized and embedded in 1% agarose plugs ($2x10^6$ cells per plug). Plugs were incubated in proteinase K digestion buffer (500 mM EDTA pH 8.0, 2% N- laurylsarcosine, and 20 mg/ml proteinase K) at 56ºC overnight. Plugs were washed with TE buffer for several hrs and then digested with RsaI and HinfI endonucleases at 37°C overnight. Plugs were loaded into 1% agarose gels for pulsed-field gel electrophoresis. After electrophoresis, gels were dried, and soaked in denaturing solution (0.2 N NaOH, 0.6 M NaCl) for 1 hr to denature DNA, followed by

neutralizing solution (1.5M NaCl, 0.5M Tris-Cl pH 7.4) for 1 hr. To detect telomere fragments, in-gel hybridization was performed using γ-^{32}P-$(CCCTAAA)_4$ oligonucleotide probe, gels were washed and exposed to a PhosphorImager screen. Telomere hybridization signals were scanned using a Typhoon PhosphorImager and quantified using ImageQuant software (GE).

ALT activity assay by monitoring C-Circle amplification

Rolling Circle Amplification (RCA) of C-circle DNA was performed as described (26), using $2x10^5$ cells per sample. The RCA reaction was carried out in 20µl reaction using 200 ng of DNA and from each samples ($1/10^{th}$) of the reaction was spotted to a Biodyne B membrane (Pall Corporation). Membranes were UV irradiated to crosslink DNA and pre-hybridized using PerfectHyb Plus hybridization buffer (Sigma-Aldrich) at 37°C for 1 hr. Membranes were hybridized with a γ-^{32}P-labelled $(CCCTAA)_3$ probe. The hybridized membrane was autoradiographed at -80°C for 1 day and developed to detect C-circle amplification products.

Statistical Analysis

All the experiments were performed at least three times in triplicates, and the data are expressed as Mean ± Standard Error Mean (SEM). Area Under the Curve (AUC) values were calculated using GraphPad Prism version 6.02 for Machintosh, GraphPad Software, San Diego California USA (www.graphpad.com). Student's t-test for two-tailed distribution with unequal variance was performed in Microsoft Excel to derive the p-values.

For synergy analyses, we used R, a system for statistical computation and graphics *(49)*, we assessed whether the combined effects from two drugs were additive (responses were equal to the sum of the single-drug effects), synergistic (greater than the sum of the single-drug effects)

or antagonistic (less than the sum of the single-drug effects) on tumor growth in a given cancer cell lines. Two-way analysis of variance (ANOVA) was used to test for the main effects of the drugs and their interaction on tumor size at the end point data for each all cell lines. Bonferroni correction was performed to counteract the problem of multiple comparisons (7). To determine whether various drug combinations exerted additive, synergistic or antagonistic impacts on decreasing tumor size, we compared the difference between observed effects with the expected additive effects for the mouse treated with both drugs (7). The difference was estimated as the interaction coefficient in the ANOVA. If there is a significant positive difference (i.e., interaction coefficient > 0 and Bonferroni adjusted p-value < 0.01), then the impact from the combined drugs was classified as antagonism. If there is a significant negative difference (i.e., interaction coefficient < 0 and Bonferroni adjusted p-value < 0.01), then the impact from the combined drugs was classified as synergistic on decreasing tumor size. If there is no significant difference, then the impact from the combined drugs was classified as additive.

Supplementary Materials and Methods references

1. Palakurthy RK, *et al.* (2009) Epigenetic silencing of the RASSF1A tumor suppressor gene through HOXB3-mediated induction of DNMT3B expression. (Translated from eng) *Mol Cell* 36(2):219-230 (in eng).
2. Santra MK, Wajapeyee N, & Green MR (2009) F-box protein FBXO31 mediates cyclin D1 degradation to induce G1 arrest after DNA damage. (Translated from eng) *Nature* 459(7247):722-725 (in eng).
3. Wajapeyee N, Serra RW, Zhu X, Mahalingam M, & Green MR (2008) Oncogenic BRAF induces senescence and apoptosis through pathways mediated by the secreted protein IGFBP7. (Translated from eng) *Cell* 132(3):363-374 (in eng).
4. Wege H, Chui MS, Le HT, Tran JM, & Zern MA (2003) SYBR Green real-time telomeric repeat amplification protocol for the rapid quantification of telomerase activity. (Translated from eng) *Nucleic Acids Res* 31(2):E3-3 (in eng).
5. Wu L, *et al.* (2006) Pot1 deficiency initiates DNA damage checkpoint activation and aberrant homologous recombination at telomeres. (Translated from eng) *Cell* 126(1):49-62 (in eng).
6. Blasco MA, *et al.* (1997) Telomere shortening and tumor formation by mouse cells lacking telomerase RNA. (Translated from eng) *Cell* 91(1):25-34 (in eng).
7. Slinker BK (1998) The statistics of synergism. (Translated from eng) *J Mol Cell Cardiol* 30(4):723-731 (in eng).

Table S1. p16 status of the telomerase positive cancer cell lines used in this study.

Cell line	Alteration in p16
ACHN	Homozygous deletion
CAKI	Homozygous deletion
HCT116	Point mutation (Premature termination codon 80 (CGA-TGA)
LOX IMVI	Homozygous deletion
NCI H460	Homozygous deletion
OVCAR5	Homozygous deletion
RKO	DNA hypermethylation of the p16 promoter
UACC62	Homozygous deletion

Table S2. Results of statistical analyses to determine synergism, antagonism and additive effects among indicated siRNA and drug combinations.

Cell line	Effect	Coefficient	p-Value	Synergism/Antagonism/Additive	Bonferroni Adjusted p-value
HCT116	Nanoparticle encapsulated p21 siRNA main effect	103.4	.00144248		1.88E-02
	Imetelstat main effect	-118.6	9.4-E-08		1.22E-06
	p21 siRNA: Imetelstat interaction	**-528.4**	**1.04E-05**	**Synergism**	**1.35E-04**
ACHN	Nanoparticle encapsulated p21 siRNA main effect	44	3.75E-22		4.88E-21
	Imetelstat main effect	-89	4.94E-26		6.24E-25
	p21 siRNA: Imetelstat interaction	**-443**	**1.09E-23**	**Synergism**	**1.42E-22**
HCT116	Sorafenib main effect	-182	2.43E-22		3.159E-21
	Imetelstat main effect	-241	5.30E-24		6.89E-23
	Sorafenib: Imetelstat interaction	**-72**	**4.23E-10**	**Synergism**	**5.499E-20**
RKO	Sorafenib main effect	-173	1.34E-33		1.742E-21
	Imetelstat main effect	-131	2.78E-21		3.614E-20
	Sorafenib: Imetelstat interaction	**-139**	**5.35E-14**	**Synergism**	**6.955E-13**
ACHN	Sorafenib main effect	-120	8.49E-20		1.1037E-18
	Imetelstat main effect	-70	5.71E-18		7.423E-17
	Sorafenib: Imetelstat interaction	**-190**	**3.44E-14**	**Synergism**	**4.472E-13**
LOXIMVI	Sorafenib main effect	-80	2.17E-20		2.82E-19
	Imetelstat main effect	-202	9.92E-24		1.29E-22
	Sorafenib: Imetelstat interaction	**-234**	**8.54E-17**	**Synergism**	**1.11E-15**
UACC62	Sorafenib main effect	-42	4.98E-19		6.47E-18
	Imetelstat main effect	-294	4.06E-25		5.28E-24
	Sorafenib: Imetelstat interaction	**-274**	**3.47E-17**	**Synergism**	**4.51E-16**
CAKI	Sorafenib main effect	-30	2.70E-20		3.15E-19
	Imetelstat main effect	-205	3.74E-25		4.86E-24
	Sorafenib: Imetelstat interaction	**-265**	**1.12E-18**	**Synergism**	**1.46E-17**
HCT116	UC2288 main effect	-90	1.18E-19		1.53E-18
	Imetelstat main effect	-295	3.57E-24		4.641E-23
	UC2288: Imetelstat interaction	**-266**	**4.27E-16**	**Synergism**	**5.55E-15**
ACHN	UC2288 main effect	-18	1.01E-19		1.313E-18
	Imetelstat main effect	-128	7.56E-23		9.828E-22
	UC2288:Imetelstat interaction	**-350**	**4.78E-19**	**Synergism**	**6.214E-18**

Table S3. Primer sequences for RT-qPCR analysis; clone ID and catalog numbers for shRNAs (Open Biosystems); antibodies used; source and concentration of chemical inhibitors used.

Application	Gene symbol	Forward primer (5′-3′)	Reverse primer (5′-3′)
RT-qPCR	*CDKN1A (p21)*	GCAGACCAGCATGACAGATTT	GGATTAGGGCTTCCTCTTGGA
	PUMA	TCGGTGCTCCTTCACTCTGG	GCAAACGAGCCCCACTCTCT
	BAX	ACCAAGGTGCCGGAACTGAT	ACTCCCGCCACAAAGATGGT
	BAK	GCCCAGGACACAGAGGAGGT	CCATGGTGCTGCTAGGTTGC
	ACTIN	GCATGGAGTCCTGTGGCATC	TTCTGCATCCTGTCGGCAAT
	E2F1	TCCCTCCTGCAGTGTCTGAA	CAGCGAGGAAGCTGACCTTT
	MDC1	GCCTTTTGACACGCACCTTG	GCCCACCCTCTCTGCTGTTT
	NBS1	TGTCAGGACGGCAGGAAAGA	TTCCCGGAGCAAAAAGAAA
	CDKN1B (p27)	GCTCCGGCTAACTCTGAGGA	AAGAATCGTCGGTTGCAGGT
	TERT	GACACACATTCCACAGGTCG	GACTCGACACCGTGTCACCTAC
	ACX	GCGCGGCTTACCCTTACCCTTACCCTAACC	
	TS	AATCCGTCGAGCAGAGTT	
	RCA	CCCTAACCCTAACCCTAA	
	Gene symbol	**Clone ID**	**Catalog number**
shRNAs	*CDKN1A (p21)*	TRCN0000040123	RHS3979-9607512
		TRCN0000040125	RHS3979-9607514
	MDC1	TRCN0000018850	RHS3979-9586172
		TRCN0000018851	RHS3979-9586173
	NBS1	TRCN0000040137	RHS3979-9607526
		TRCN0000010393	RHS3979-9630894
	E2F1	TRCN0000000251	RHS3979-9568611
		TRCN0000000253	RHS3979-9568613
	PUMA	TRCN0000033611	RHS3979-9601019
	CDKN1B	TRCN0000039929	RHS3979-9607318
		TRCN0000009856	RHS3979-97079654
siRNA	**Gene symbol**		**Sequence**
	CDKN1A (p21)	Thermoscientific	GCGAUGGAACUUCGACUUU
	Non-targeting	Thermoscientific	UAAGGCUAUGAAGAGAUAC
	Protein symbol	**Antibody source**	
Immunoblot/	CDKN1A (p21)	Santa Cruz Biotechnology, Inc.	
ChIP	PUMA	Thermo Scientific	
	BAX	Santa Cruz Biotechnology, Inc.	
	BAK	Santa Cruz Biotechnology, Inc.	
	TERT	R & D Systems	
	p53	Santa Cruz Biotechnology, Inc.	
	Cleaved caspase 3	Cell signaling	
	Actin	Sigma-Aldrich	
	Inhibitor	**Concentration**	**Source**
	Imetelstat	2.5 μM	Geron Corporation
	Mismatch Oligonucleotide	2.5 μM	Geron Corporation

	Sorafenib	1 μM and 2.5 μM	LC Laboratories
	UC2288	1 μM, 2.5 μM and 5 μM	
	CP-31398	2 and 5 μg/ml	Sigma-Aldrich

Supplementary figure legends

Fig. S1. shRNA-mediated inhibition of *TERT* expression leads to potent growth inhibition in HCT116 p21KO cells. Analysis of HCT116 p21KO (*A–D*) or wild-type (*E–H*) cells stably transduced with non-specific control (NS) or two different *TERT* shRNAs. (*A, E*) qRT-PCR analysis of *TERT* mRNA. (*B, F*) Cell viability as measured by trypan blue exclusion assay. Cell viability relative to non-specific shRNA is plotted. (*C, G*) Annexin V-FITC positive cells were quantified by FACS analysis. % Annexin V-FITC positive cells are plotted. (*D, H*) Telomerase activity as measured by the TRAP assay and plotted relative to the mismatch oligonucleotide. *** represents $p<0.0001$.

Fig. S2. shRNA-mediated loss of *p21* leads to apoptosis induction upon telomerase inhibition. Analysis of HCT116 cells stably transduced with non-specific control (NS) or two different *p21* shRNAs. (*A*) Immunoblot analysis of p21 protein. (*B*) qRT-PCR analysis of *p21* mRNA. (*C-F*) Cells were treated with mismatch oligonucleotide or with imetelstat for 6 weeks. (*C*) Colony formation monitored by crystal violet staining. (*D*) Cell viability as measured by trypan blue exclusion assay. Cell viability relative to mismatch oligonucleotide is plotted. (*E*) Apoptosis monitored by FACS analysis. (*F*) Annexin V-FITC positive cells were quantified using FACS analysis. % Annexin V-FITC positive cells are plotted. (*G*) Telomerase activity as measured by the TRAP assay and plotted relative to the mismatch oligonucleotide. ** and *** represents $p<0.001$ and $p<0.0001$ respectively.

Fig. S3. shRNA-mediated *p21* knockdown in unrelated human cancer cell lines sensitize them to telomerase inhibition-mediated apoptosis. (*A, B*) Immunoblot analysis of RKO (*A*) and ACHN (*B*) cells stably transduced with non-specific control (NS) or two different *p21* shRNAs. (*C*) (Left) *p21* gene specific probes intensity values for the indicated cell lines were obtained from BioGPS, Relative *p21* expression is plotted. (Right) Immunoblot analysis to monitor p21 expression levels in the indicated cell lines. Actin was used as a loading control. (*D-F*) Indicated cells were treated with mismatch oligonucleotide or with imetelstat for 6 weeks. (*D*) Cell viability was measured by trypan blue exclusion assay. Cell viability relative to mismatch oligonucleotide is plotted. (*E*) Annexin V-FITC positive cells were quantified for indicated cell lines using FACS analyses. % Annexin V positive cells under indicated conditions is plotted. (*F*) Telomerase activity as measured by the TRAP assay and plotted relative to the mismatch oligonucleotide. (*G*) Dot blot analysis of rolling circle amplification of C-circle DNA to measure ALT activity in the indicated cell lines. ** and *** represents $p<0.001$ and $p<0.0001$ respectively.

Fig. S4. Loss of checkpoint proteins MDC1 or NBS1 do not cooperate with telomerase inhibition to induce growth arrest. HCT116 cells stably transduced with *MDC1* (*A–F*) or *NBS1* (*G–L*) shRNAs. Where indicated, cells were treated either with mismatch oligonucleotide or imetelstat for 6 weeks. (*A, G*) qRT-PCR analysis of *MDC1* (*A*) or *NBS1* (*G*) mRNA. (*B, H*) Colony formation monitored by crystal violet staining. (*C, I*) Cell viability as measured by trypan blue exclusion assay. Cell viability relative to mismatch oligonucleotide is plotted. (*D, J*) Apoptosis monitored by FACS analysis. (*E, K*) Telomerase activity as measured by the TRAP

assay and plotted relative to the mismatch oligonucleotide. (*F, L*) qRT-PCR analysis of *PUMA* mRNA. *** represents $p<0.0001$.

Fig. S5. Loss of cyclin dependent kinase inhibitor p27 does not cooperate with telomerase inhibition to induce growth arrest. HCT116 cells stably transduced with *p27* shRNAs and where indicated, cells were treated either with mismatch oligonucleotide or imetelstat for 6 weeks. (*A*) qRT-PCR analysis of *p27* mRNA. (*B*) Colony formation monitored by crystal violet staining. (*C*) Cell viability as measured by trypan blue exclusion assay. Cell viability relative to mismatch oligonucleotide is plotted. (*D*) Apoptosis monitored by FACS analysis of sub G1 population. (*E*) Telomerase activity as measured by the TRAP assay and plotted relative to the mismatch oligonucleotide. (*F*) qRT-PCR analysis of *PUMA* mRNA.

Fig. S6. ER-stress inducer tunicamycin does not enhance tumor cell growth after Imetelstat treatment or loss of p21. (*A*) Relative cell viability measured by trypan blue exclusion assay of HCT116 cells that were either remained untreated or treated with imetelstat, tunicamycin or both. (*B*) Apoptosis was measured by Annexin V-FITC staining for HCT116 cells that were either remained untreated or treated with imetelstat, tunicamycin or both. (*C*) Relative cell viability measured by trypan blue exclusion assay of HCT116 wild type or p21 KO cells that were either remained untreated or treated with tunicamycin. (*D*) Apoptosis was measured by Annexin V-FITC staining for HCT116 wild type or p21 KO cells that were either remained untreated or treated with tunicamycin.

Fig. S7. *p21* does not regulate the ability of imetelstat to inhibit telomerase activity, telomere shortening or ALT. Indicated cell lines were treated with mismatch oligonucleotide or imetelstat for 6 weeks. (*A*) Southern blot to measure telomere length. Size markers in kilobase are shown next to the gel image. (*B*) Telomere length relative to HCT116 cells treated with mismatch oligonucleotide, in all indicated cell lines corresponding to (*A*) is presented. (*C*) Telomere PNA-FISH to monitor signal-free chromosomal ends. (*D*) Signal-free chromosomal ends in (*C*) were quantified and plotted relative to mismatch oligonucleotide. (*E*) Dot blot analysis of rolling circle amplification of C-circle DNA to measure ALT activity in the indicated cell lines. ** represents $p<0.001$.

Fig. S8. Treatment of ALT activated cell line U2OS with imetelstat did not induce growth inhibition irrespective of p21 expression. (*A, B*) U2OS cells expressing indicated shRNAs were treated with either a mismatch oligonucleotide or with Imetelstat for 6 weeks. (*A*) Colony formation was monitored by crystal violet staining. (*B*) cell viability was measured by trypan blue exclusion assay

Fig. S9. *PUMA* activation is a general requirement for telomerase inhibition-induced tumor suppression. (*A, B*) RKO cells with indicated shRNAs were treated with either a mismatch oligonucleotide or imetelstat for 6 weeks. (*A*) Fold change in *PUMA* transcript levels measured by qRT-PCR (*B*) Immunoblot analysis was performed for indicated proteins. (*C*) *PUMA* knockdown in *p21* shRNA expressing RKO cells was confirmed by qRT-PCR. (*D-F*) RKO cells with indicated shRNAs were treated with either a mismatch oligonucleotide or imetelstat for 6 weeks. (*D*) Relative cell viability was measured by trypan blue exclusion assay.

(*E*) Annexin V-FITC positive cells were quantified using FACS analysis. % Annexin V-FITC positive cells are plotted. (*F*) Relative telomerase activities of indicated cells. (*G, H*) ACHN cells with indicated shRNAs were treated with either a mismatch oligonucleotide or imetelstat for 6 weeks. (*G*) Fold change in *PUMA* transcript levels measured by qRT-PCR. (*H*) Immunoblot analysis was performed for indicated proteins. *(I*) *PUMA* knockdown in *p21* shRNA expressing ACHN cells was confirmed by qRT-PCR. (*J-L*) ACHN cells with indicated shRNAs were treated with either a mismatch oligonucleotide or imetelstat for 6 weeks. (*J*) Cell viability was measured by trypan blue exclusion assay. (*K*) Annexin V-FITC positive cells were quantified using FACS analysis. % Annexin V-FITC positive cells are plotted. (*L*) Relative telomerase activities of indicated cells. ** represents $p<0.001$.

Fig. S10. Analyses of telomerase activity by TRAP assay. (*A*) Relative telomerase activities of HCT116 p21KO cells expressing indicated shRNAs and treated with a mismatch oligonucleotide (-) or with imetelstat (+). (*B*) Relative telomerase activities of HCT116 wild type and p53KO cells treated with a mismatch oligonucleotide (-) or with imetelstat (+).

Fig. S11. Telomerase inhibition-induces strong tumor suppression in cancer cells with lower *p21* expression in a *PUMA* dependent manner. (*A*) Indicated cell lines were treated with either a mismatch oligonucleotide or imetelstat for 6 weeks. Fold change in *PUMA* transcript levels measured by qRT-PCR. (*B*) *PUMA* knockdown in NCI H460 and OVCAR5 cells was confirmed by qRT-PCR. (*C, D*) Indicated cell lines were treated with either a mismatch oligonucleotide or imetelstat. (*C*) Cell viability was measured by trypan blue exclusion assay.

(*D*) Relative telomerase activities of indicated cells. * and ** represents $p<0.01$ and $p<0.001$ respectively.

Fig. S12. Nanoparticle-based systemic p21 siRNA delivery inhibits the growth of tumors in combination with imetelstat treatment. (*A*) HCT116 cells were injected into the flanks of nude mice and were treated as indicated. Tumor volumes at indicated days are shown and the representative tumors are presented. (*B*) ACHN cells were injected into the flanks of nude mice and were treated as indicated. Tumor volumes at indicated days are shown and the representative tumors are presented. (*C*) Mouse derived HCT116 xenograft tumor under indicated treatment conditions were analyzed for indicated proteins by immunoblot analysis. (*D*) Mouse derived ACHN xenograft tumor under indicated treatment conditions were analyzed for indicated proteins by immunoblot analysis. (*E*) Mouse derived HCT116 xenograft tumor under indicated treatment conditions were analyzed for telomerase activity by TRAP assay. (*F*) Mouse derived ACHN xenograft tumor under indicated treatment conditions were analyzed for telomerase activity by TRAP assay. * , **, *** represents $p<0.01$, $p<0.001$, $p<0.0001$ respectively

Fig. S13. Analyses of the drug toxicity of sorafinib, imetelstat and their combination in mice. (*A*) Control mice group bearing HCT116 tumors or HCT116 tumor bearing mice treated with the indicated drugs were weighed at the end of the experiment. Average reduction in body weight in drug treatment group is plotted in comparison to control mice. (*B*) Activities of alanine aminotransferase (ALT), aspartate aminotransferase (AST) and alkaline phosphatase (AP) were analyzed in the sera of the indicated mice groups. Activities of these enzymes in comparison to the control mice group is plotted. (*C*) Relative hemacrite (packed red cell volume) level in

HCT116 tumor bearing mice, compared to vehicle control. (*D*) Relative Red Blood cell (RBC) count in HCT116 tumor bearing mice under indicated condition, compared to vehicle control. (*E*) Relative White blood cell (WBC) count in HCT116 tumor bearing mice under indicated condition, compared to vehicle control. (*F*) Activity of creatinine in the sera of the indicated mice groups. Activities in comparison to the control mice group is plotted.

Fig. S14. Simultaneous inhibition of telomerase and p21 cause synergistic tumor suppression in a wide variety of cancer cells. (*A*-*E*) Average tumor volumes from mice treated with vehicle, sorafenib alone, imetelstat alone or with both drugs for indicated cell lines. *** represents $p<0.0001$.

Fig. S15. Analyses of the drug toxicity of UC2288, imetelstat and their combination in mice. (*A*) Control mice group bearing HCT116 tumors or HCT116 tumor bearing mice treated with the indicated drugs were weighed at the end of the experiment. Average reduction in body weight in drug treatment group is plotted in comparison to control mice. (*B*) Activities of alanine aminotransferase (ALT), aspartate aminotransferase (AST) and alkaline phosphatase (AP) were analyzed in the sera of the indicated mice groups. Activities of these enzymes in comparison to the control mice group is plotted. (*C*) Relative hemacrite (packed red cell volume) level in HCT116 tumor bearing mice, compared to vehicle control. (*D*) Relative Red Blood cell (RBC) count in HCT116 tumor bearing mice under indicated condition, compared to vehicle control. (*E*) Relative White blood cell (WBC) count in HCT116 tumor bearing mice under indicated condition, compared to vehicle control. (*F*) Activity of creatinine in the sera of the indicated mice groups. Activities in comparison to the control mice group, is plotted.

Fig. S16. Telomerase activity measurement. DLD1 (**Left**) and A375.S2 (**Right**) cells treated as indicated were analyzed for telomerase activity. Relative telomerase activity is plotted.

Fig. S1

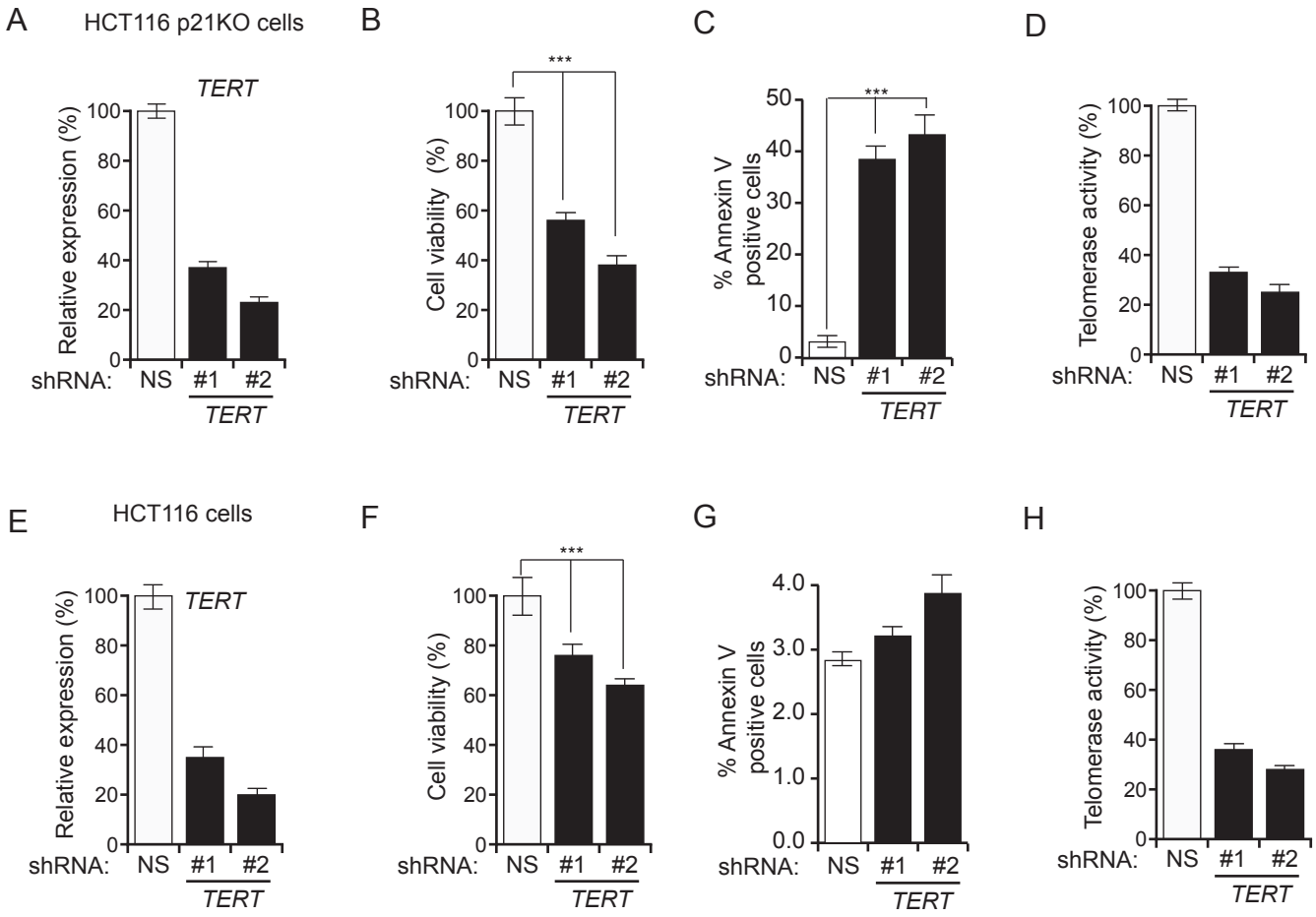
A
HCT116 p21KO cells
TERT
Relative expression (%)
100
80
60
40
20
0
shRNA:
NS
#1
#2
TERT
B
***
Cell viability (%)
C
% Annexin V positive cells
50
40
30
20
10
0
D
Telomerase activity (%)
E
HCT116 cells
F
G
4.0
3.0
2.0
1.0
0.0
H

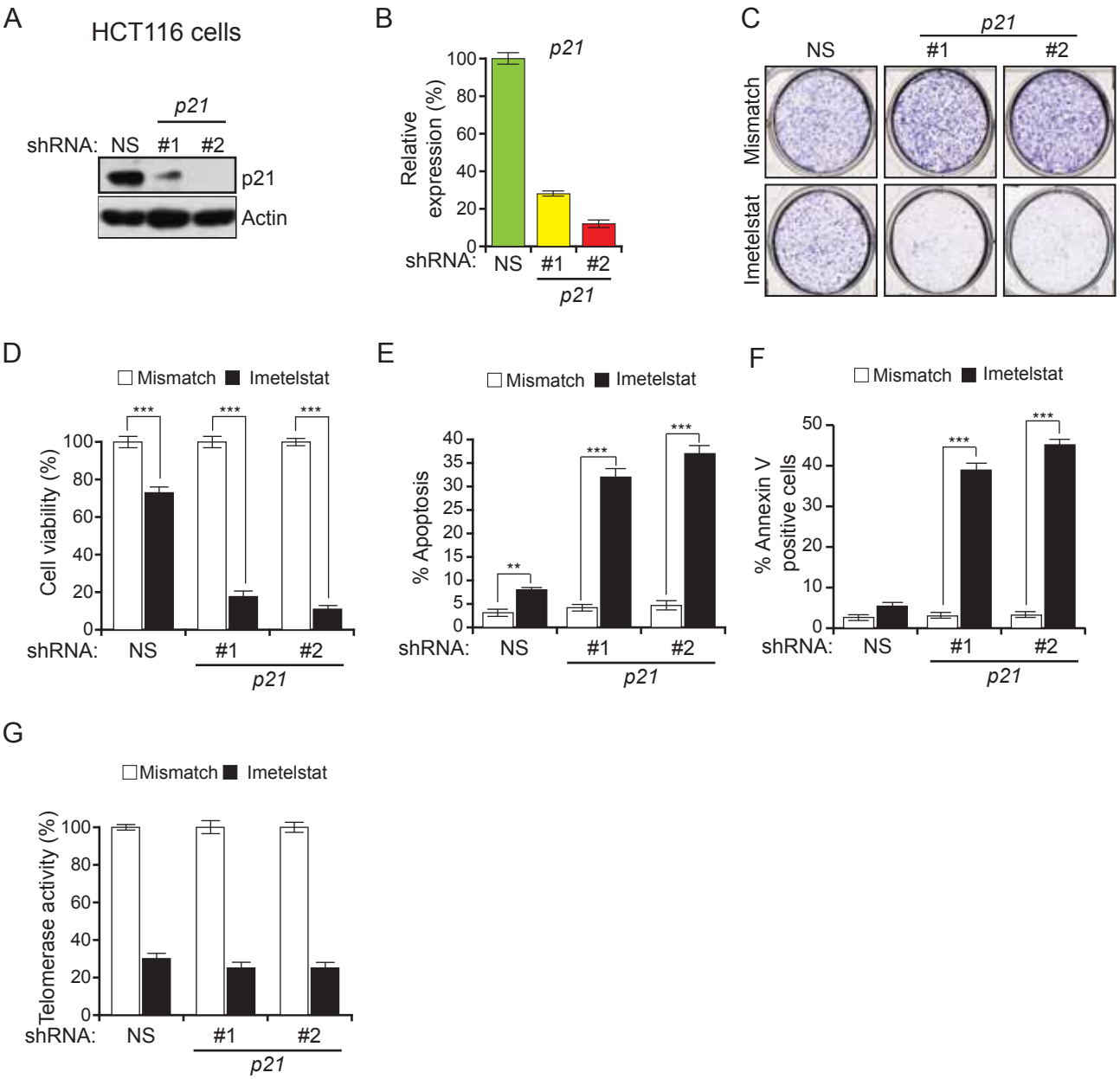
A
HCT116 cells
p21
shRNA: NS #1 #2
p21
Actin
B
p21
Relative expression (%)
100
80
60
40
20
0
shRNA: NS #1 #2
p21
C
p21
NS #1 #2
Mismatch
Imetelstat
D
Mismatch Imetelstat
Cell viability (%)
***
shRNA: NS #1 #2
p21
E
Mismatch Imetelstat
% Apoptosis
**
***
shRNA: NS #1 #2
p21
F
Mismatch Imetelstat
% Annexin V positive cells
***
shRNA: NS #1 #2
p21
G
Mismatch Imetelstat
Telomerase activity (%)
shRNA: NS #1 #2
p21

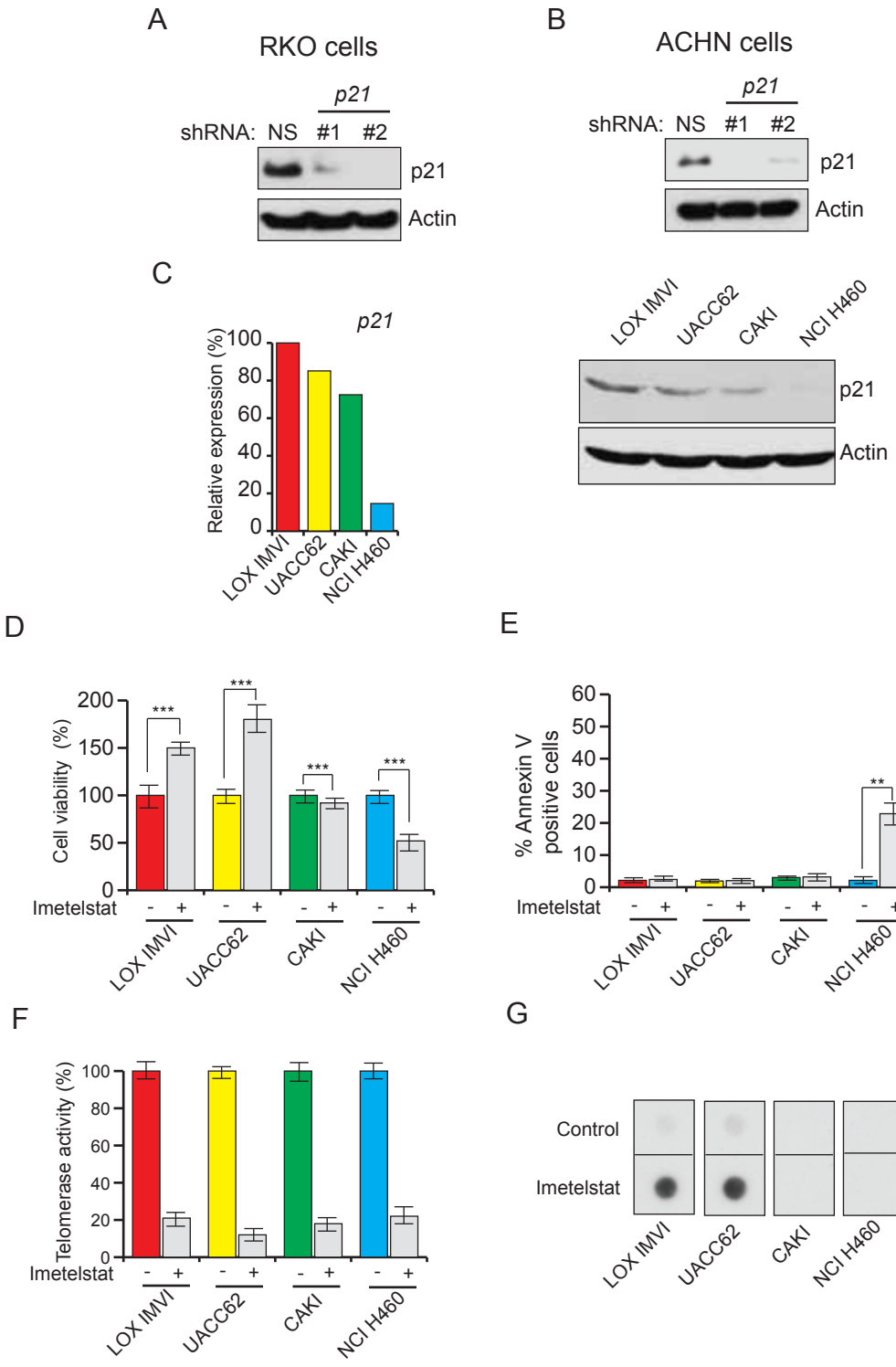
A
RKO cells
p21
shRNA: NS #1 #2
p21
Actin
B
ACHN cells
p21
shRNA: NS #1 #2
p21
Actin
C
p21
Relative expression (%)
100
80
60
40
20
0
LOX IMVI
UACC62
CAKI
NCI H460
LOX IMVI
UACC62
CAKI
NCI H460
p21
Actin
D
Cell viability (%)
200
150
100
50
0
***
***
***
***
Imetelstat
- + - + - + - +
LOX IMVI
UACC62
CAKI
NCI H460
E
% Annexin V positive cells
60
50
40
30
20
10
0
**
Imetelstat
- + - + - + - +
LOX IMVI
UACC62
CAKI
NCI H460
F
Telomerase activity (%)
100
80
60
40
20
0
Imetelstat
- + - + - + - +
LOX IMVI
UACC62
CAKI
NCI H460
G
Control
Imetelstat
LOX IMVI
UACC62
CAKI
NCI H460

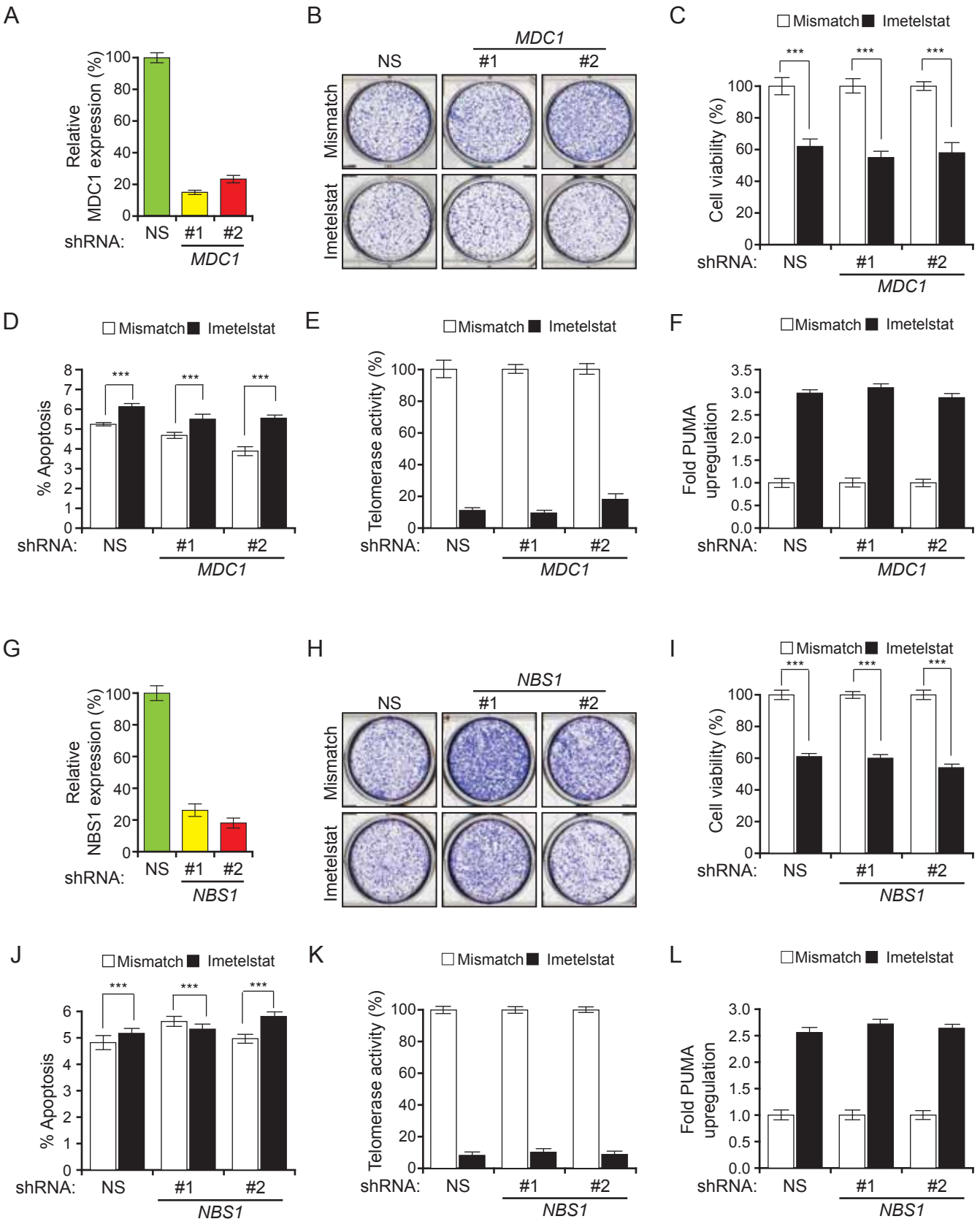
A
Relative MDC1 expression (%)
100
80
60
40
20
0
shRNA:
NS
#1
#2
MDC1
B
MDC1
NS
#1
#2
Mismatch
Imetelstat
C
Mismatch
Imetelstat
***
Cell viability (%)
shRNA:
NS
#1
#2
MDC1
D
Mismatch
Imetelstat
% Apoptosis
8
7
6
5
4
3
2
1
0
***
shRNA:
NS
#1
#2
MDC1
E
Mismatch
Imetelstat
Telomerase activity (%)
shRNA:
NS
#1
#2
MDC1
F
Mismatch
Imetelstat
Fold PUMA upregulation
3.5
3.0
2.5
2.0
1.5
1.0
0.5
0.0
shRNA:
NS
#1
#2
MDC1
G
Relative NBS1 expression (%)
shRNA:
NS
#1
#2
NBS1
H
NBS1
NS
#1
#2
Mismatch
Imetelstat
I
Mismatch
Imetelstat
Cell viability (%)
shRNA:
NS
#1
#2
NBS1
J
Mismatch
Imetelstat
% Apoptosis
shRNA:
NS
#1
#2
NBS1
K
Mismatch
Imetelstat
Telomerase activity (%)
shRNA:
NS
#1
#2
NBS1
L
Mismatch
Imetelstat
Fold PUMA upregulation
shRNA:
NS
#1
#2
NBS1

Fig. S5

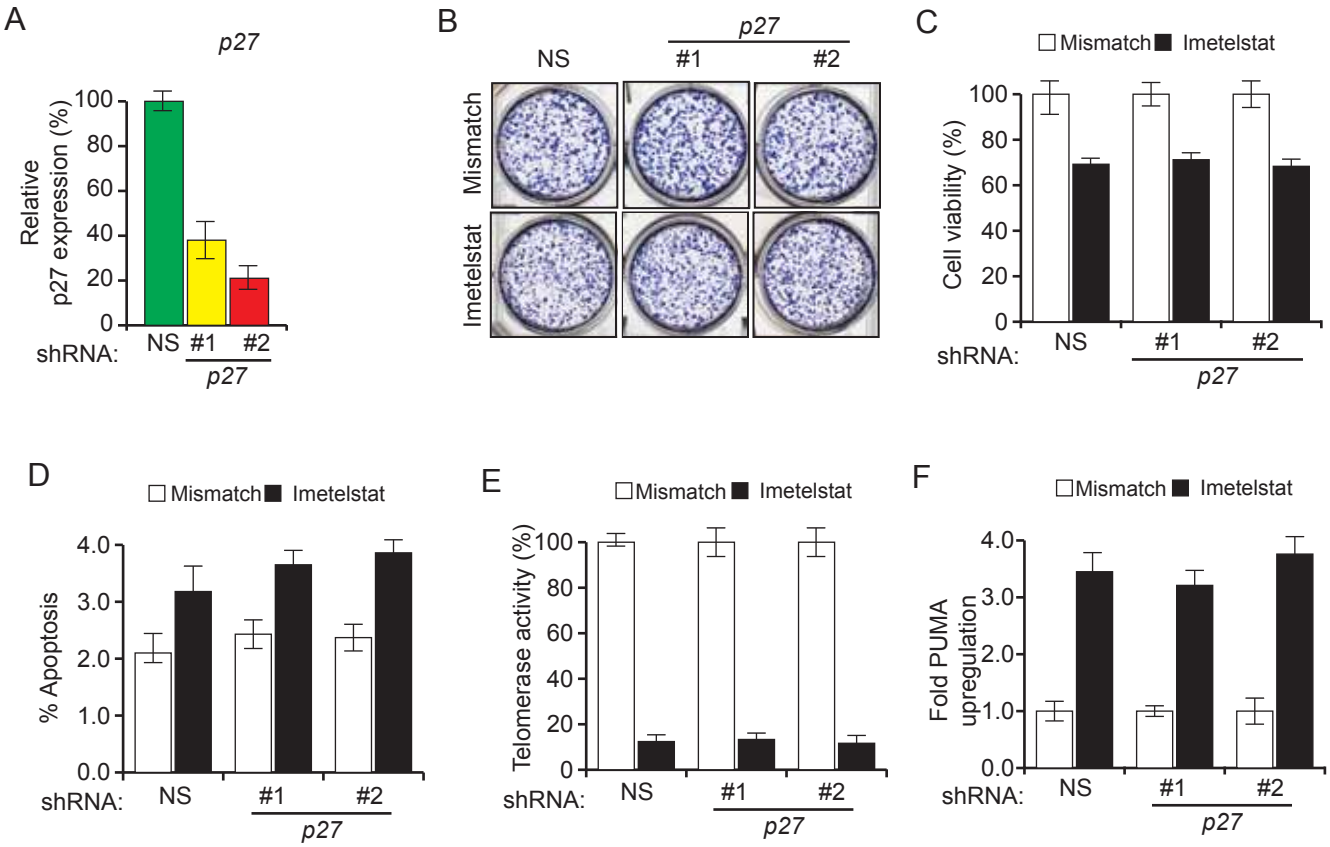
A
p27
Relative p27 expression (%)
100
80
60
40
20
0
shRNA:
NS
#1
#2
p27
B
p27
NS
#1
#2
Mismatch
Imetelstat
C
Mismatch
Imetelstat
Cell viability (%)
100
80
60
40
20
0
shRNA:
NS
#1
#2
p27
D
Mismatch
Imetelstat
% Apoptosis
4.0
3.0
2.0
1.0
0.0
shRNA:
NS
#1
#2
p27
E
Mismatch
Imetelstat
Telomerase activity (%)
100
80
60
40
20
0
shRNA:
NS
#1
#2
p27
F
Mismatch
Imetelstat
Fold PUMA upregulation
4.0
3.0
2.0
1.0
0.0
shRNA:
NS
#1
#2
p27

Fig. S6

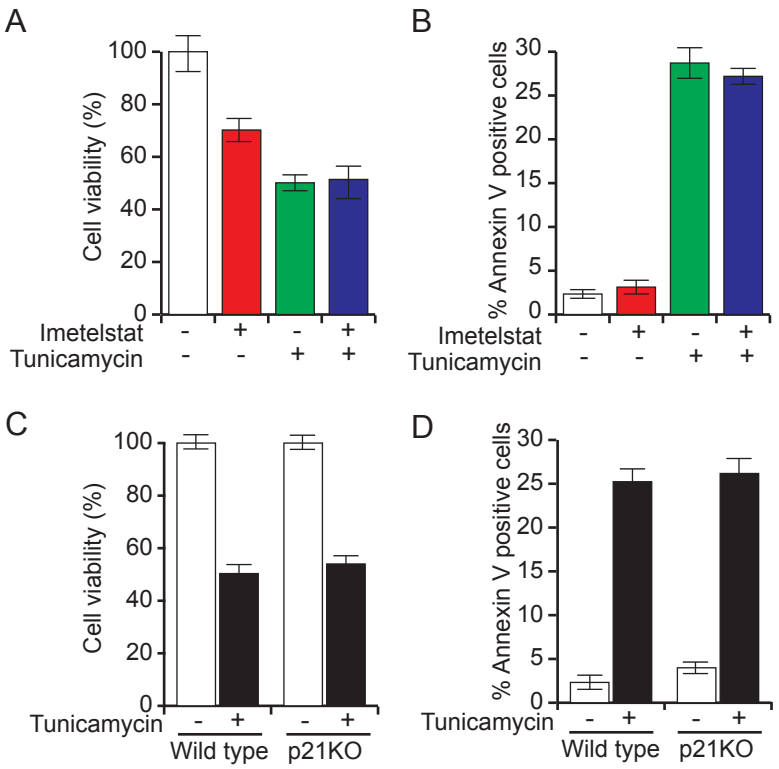
A
Cell viability (%)
100
80
60
40
20
0
Imetelstat - + - +
Tunicamycin - - + +
B
% Annexin V positive cells
30
25
20
15
10
5
0
Imetelstat - + - +
Tunicamycin - - + +
C
Cell viability (%)
100
80
60
40
20
0
Tunicamycin - + - +
Wild type
p21KO
D
% Annexin V positive cells
30
25
20
15
10
5
0
Tunicamycin - + - +
Wild type
p21KO

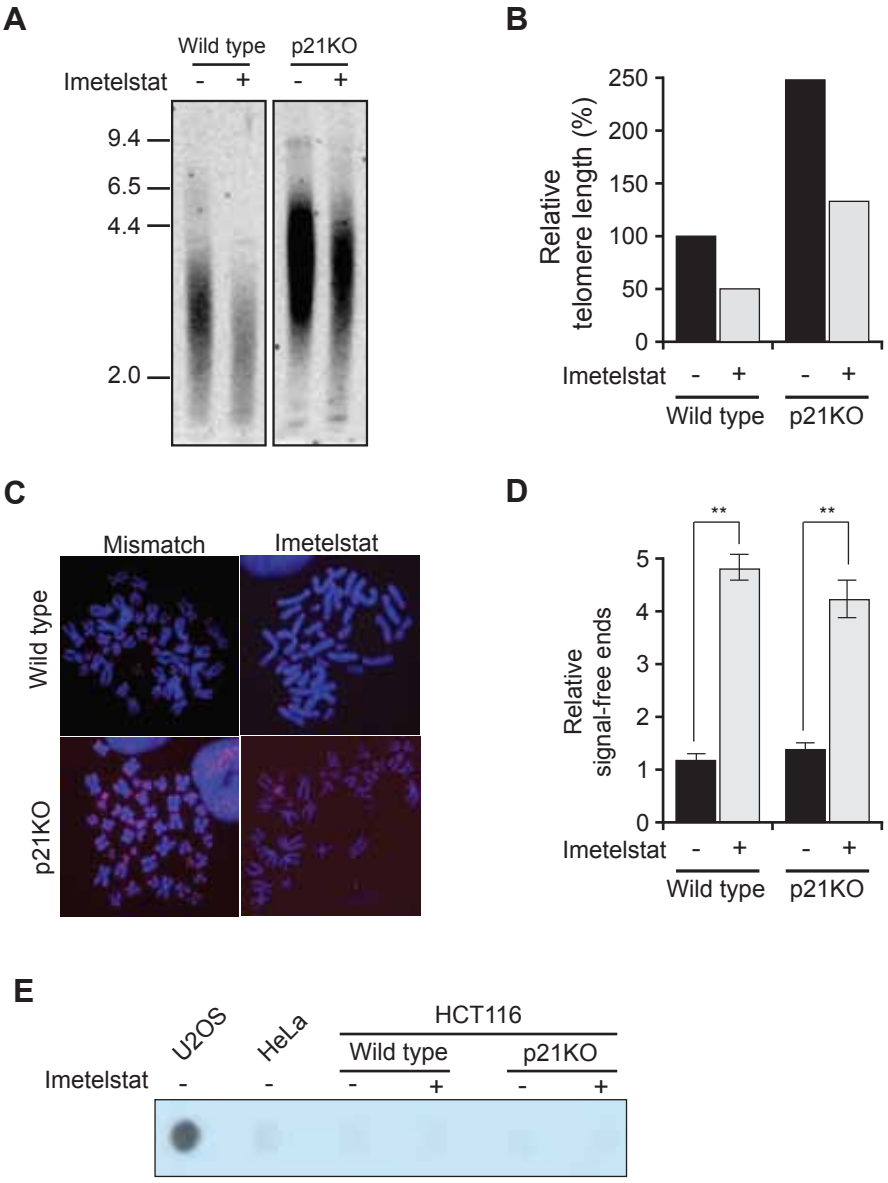
A
Wild type
p21KO
Imetelstat
- + - +
9.4
6.5
4.4
2.0
B
Relative telomere length (%)
250
200
150
100
50
0
Imetelstat - + - +
Wild type
p21KO
C
Mismatch
Imetelstat
Wild type
p21KO
D
Relative signal-free ends
**
**
5
4
3
2
1
0
Imetelstat - + - +
Wild type
p21KO
E
U2OS
HeLa
HCT116
Wild type
p21KO
Imetelstat
- - - + - +

Fig. S8

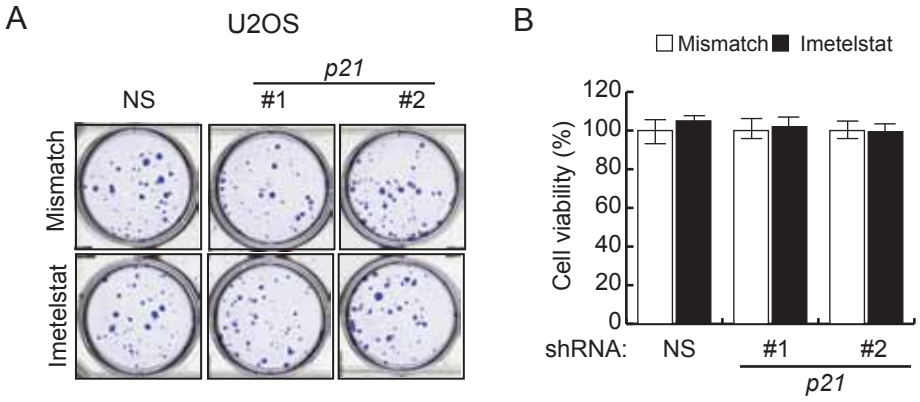
A
U2OS
p21
NS
#1
#2
Mismatch
Imetelstat
B
Mismatch
Imetelstat
Cell viability (%)
120
100
80
60
40
20
0
shRNA:
NS
#1
#2
p21

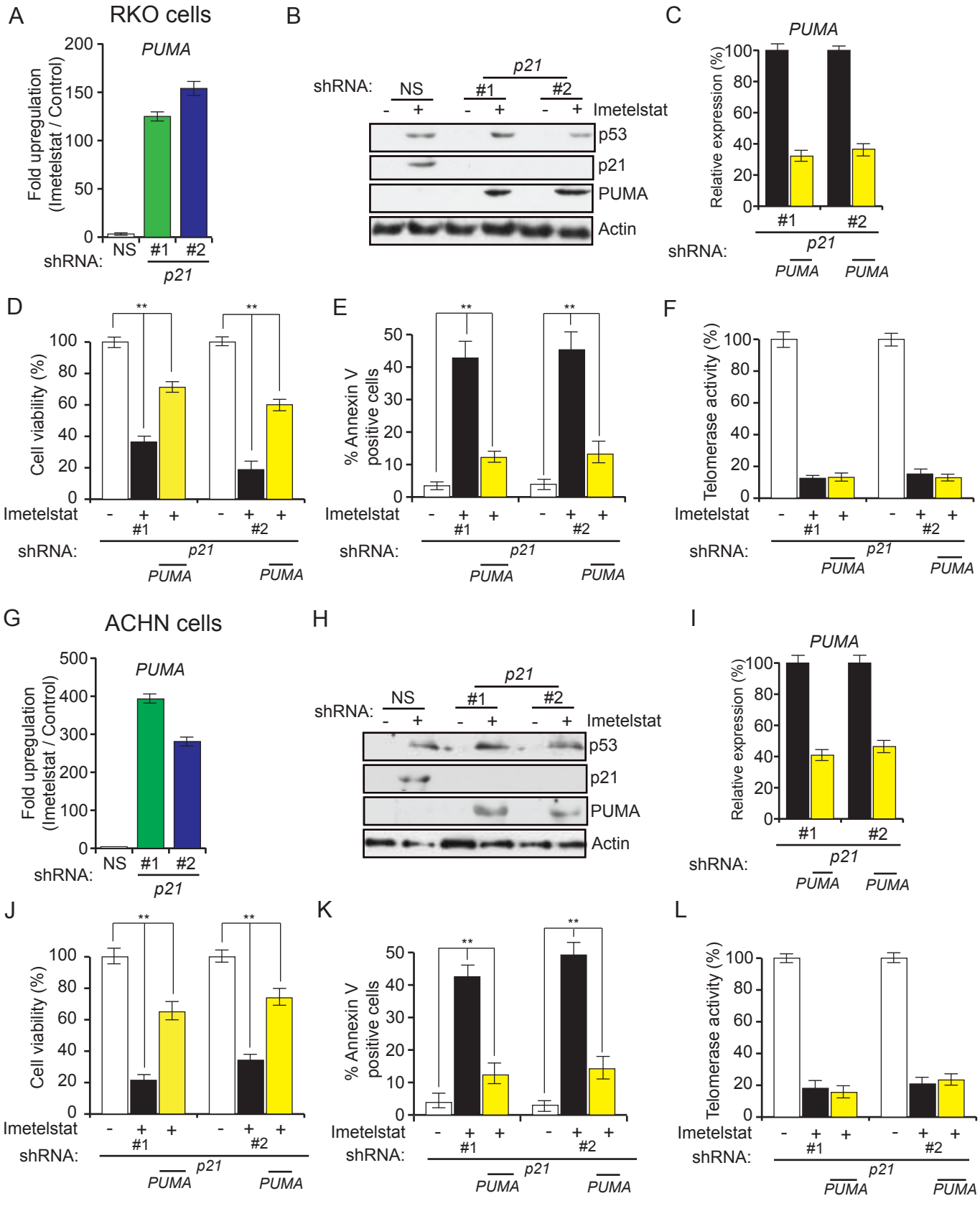
A
RKO cells
PUMA
Fold upregulation (Imetelstat / Control)
200
150
100
50
0
NS
#1
#2
shRNA:
p21
B
shRNA:
NS
p21
#1
#2
Imetelstat
p53
p21
PUMA
Actin
C
PUMA
Relative expression (%)
100
80
60
40
20
0
#1
#2
shRNA:
p21
PUMA
PUMA
D
Cell viability (%)
100
80
60
40
20
0
**
**
Imetelstat
shRNA:
#1
#2
p21
PUMA
PUMA
E
% Annexin V positive cells
50
40
30
20
10
0
**
**
Imetelstat
shRNA:
#1
#2
p21
PUMA
PUMA
F
Telomerase activity (%)
100
80
60
40
20
0
Imetelstat
shRNA:
#1
#2
p21
PUMA
PUMA
G
ACHN cells
PUMA
Fold upregulation (Imetelstat / Control)
500
400
300
200
100
0
NS
#1
#2
shRNA:
p21
H
shRNA:
NS
p21
#1
#2
Imetelstat
p53
p21
PUMA
Actin
I
PUMA
Relative expression (%)
100
80
60
40
20
0
#1
#2
shRNA:
p21
PUMA
PUMA
J
Cell viability (%)
100
80
60
40
20
0
**
**
Imetelstat
shRNA:
#1
#2
p21
PUMA
PUMA
K
% Annexin V positive cells
50
40
30
20
10
0
**
**
Imetelstat
shRNA:
#1
#2
p21
PUMA
PUMA
L
Telomerase activity (%)
100
80
60
40
20
0
Imetelstat
shRNA:
#1
#2
p21
PUMA
PUMA

Fig. S10

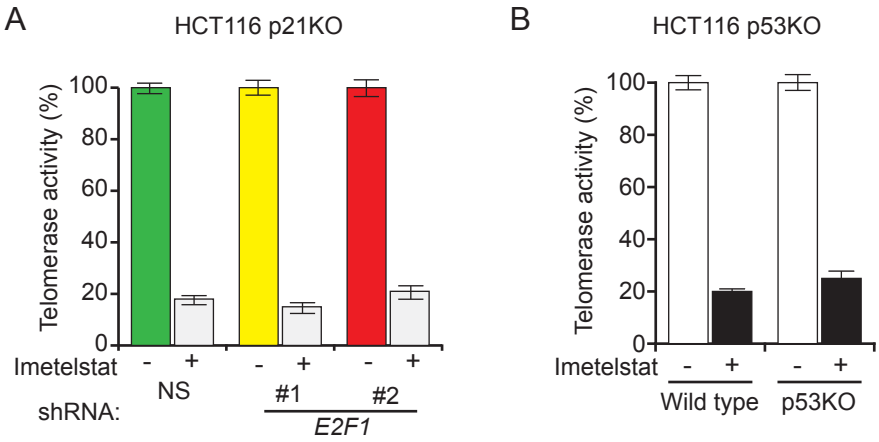
A
HCT116 p21KO
Telomerase activity (%)
100
80
60
40
20
0
Imetelstat
-
+
-
+
-
+
NS
#1
#2
shRNA:
E2F1
B
HCT116 p53KO
Telomerase activity (%)
100
80
60
40
20
0
Imetelstat
-
+
-
+
Wild type
p53KO

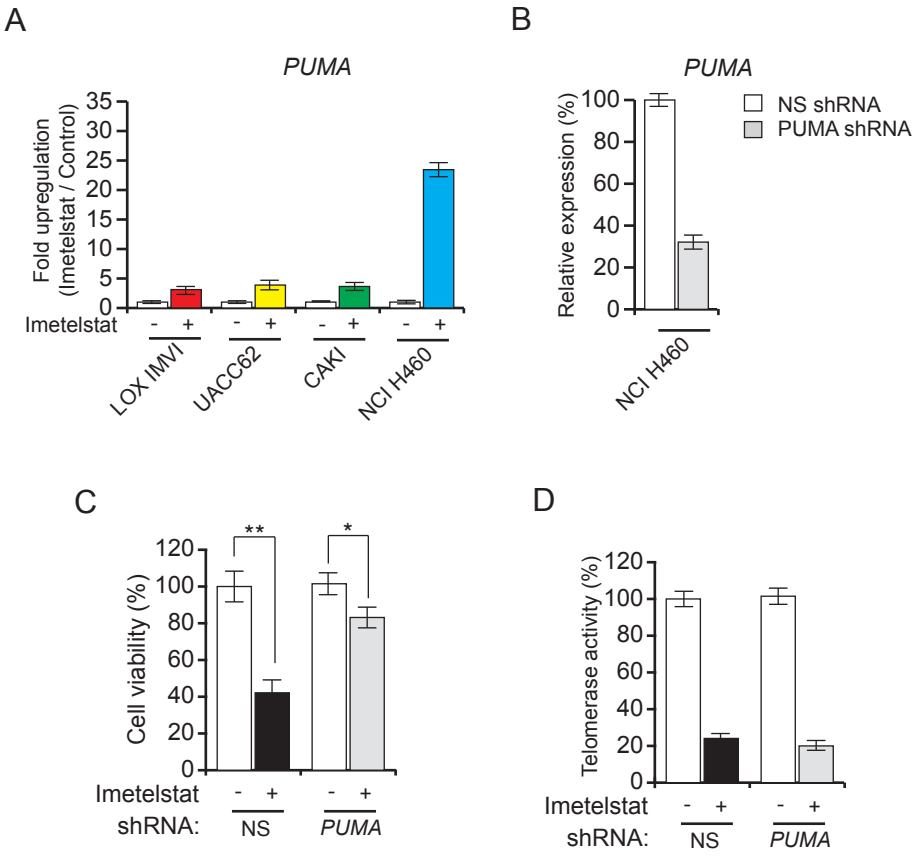
A
PUMA
Fold upregulation (Imetelstat / Control)
35
30
25
20
15
10
5
0
Imetelstat
- + - + - + - +
LOX IMVI
UACC62
CAKI
NCI H460
B
PUMA
Relative expression (%)
100
80
60
40
20
0
NS shRNA
PUMA shRNA
NCI H460
C
Cell viability (%)
120
100
80
60
40
20
0
**
*
Imetelstat
shRNA:
- + - +
NS
PUMA
D
Telomerase activity (%)
120
100
80
60
40
20
0
Imetelstat
shRNA:
- + - +
NS
PUMA

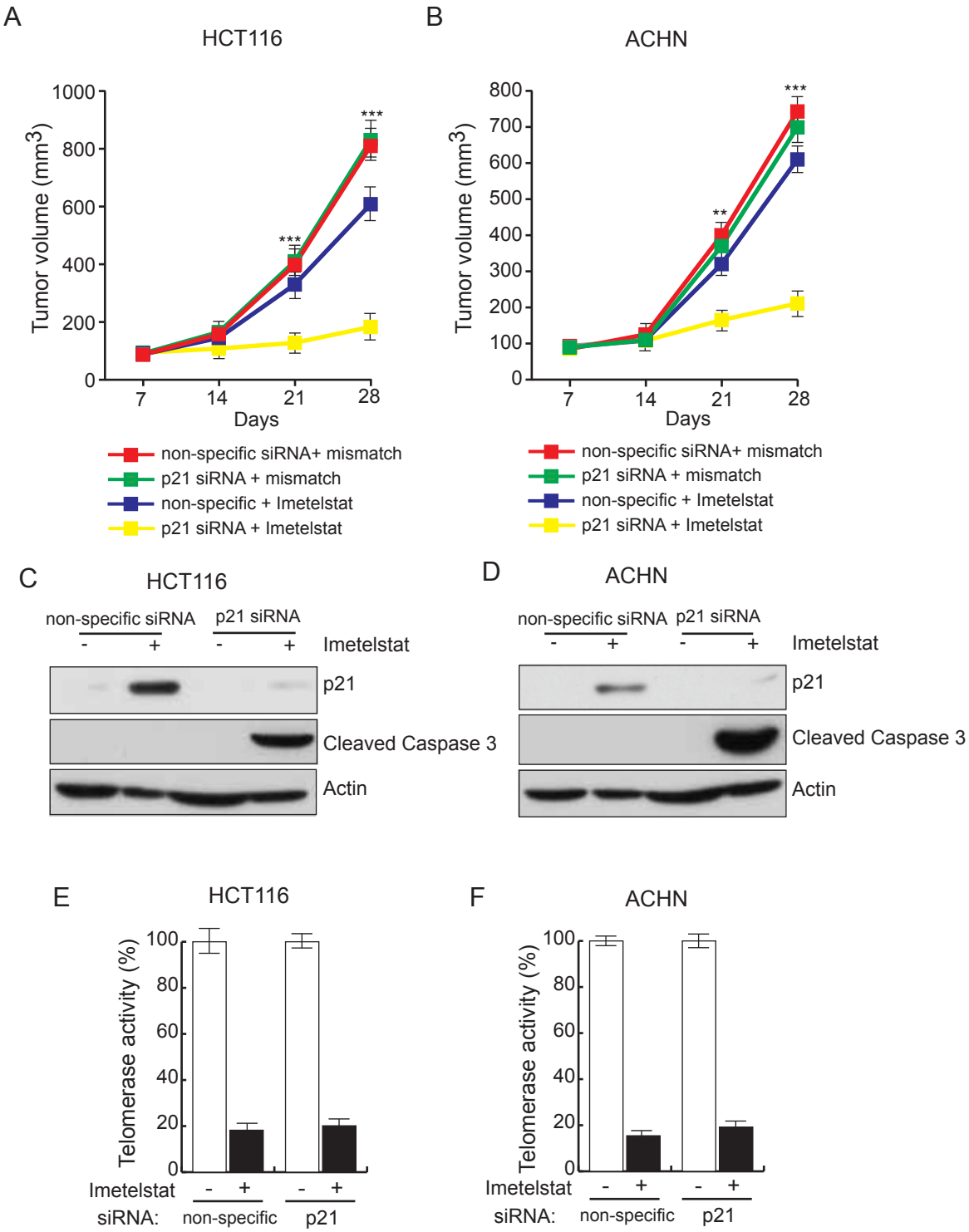
A
HCT116
Tumor volume (mm3)
Days
non-specific siRNA+ mismatch
p21 siRNA + mismatch
non-specific + Imetelstat
p21 siRNA + Imetelstat
B
ACHN
C
HCT116
non-specific siRNA
p21 siRNA
Imetelstat
p21
Cleaved Caspase 3
Actin
D
ACHN
E
HCT116
Telomerase activity (%)
siRNA:
non-specific
p21
F
ACHN

Fig. S13

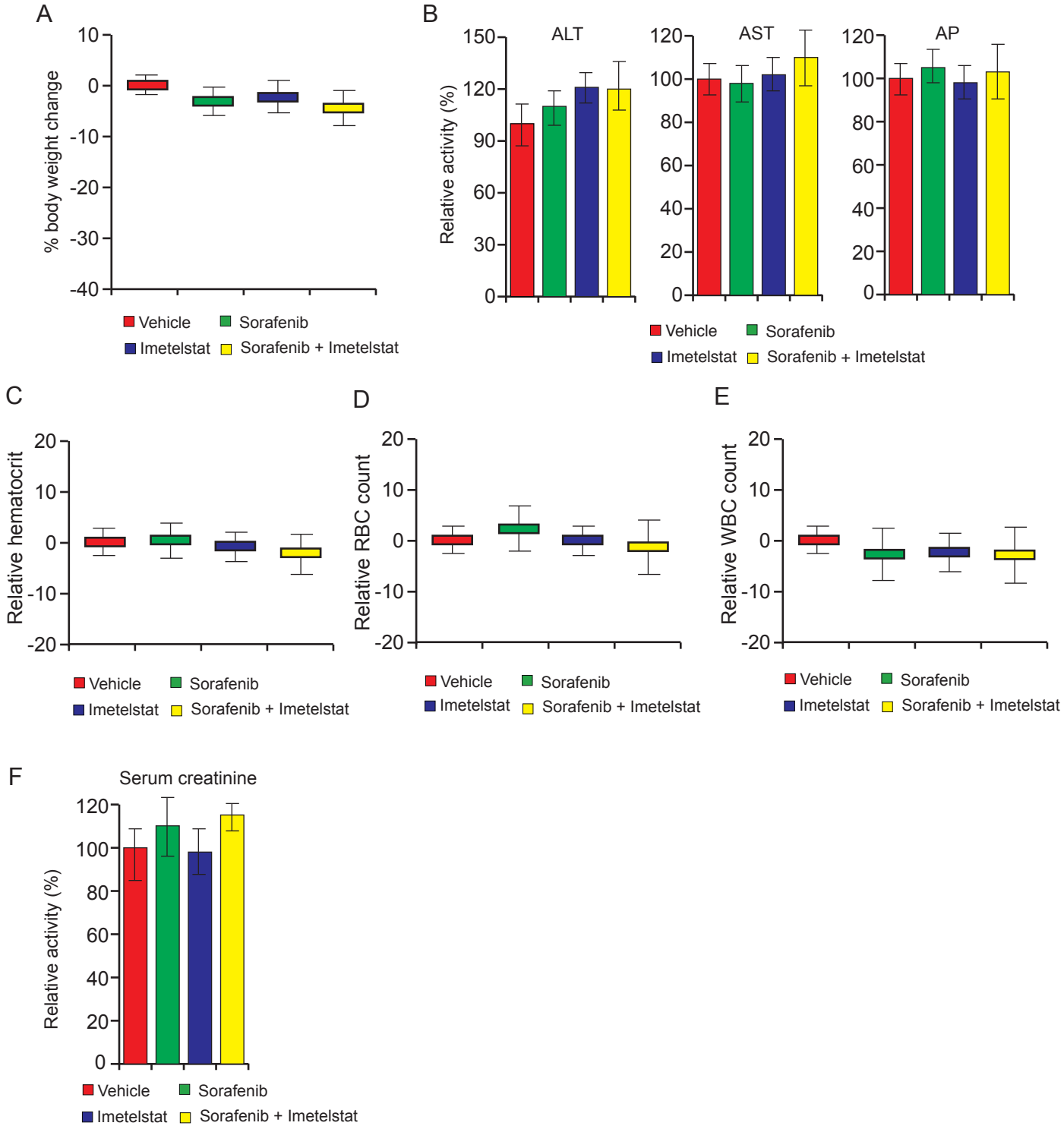
A
% body weight change
10
0
-10
-20
-30
-40
Vehicle
Sorafenib
Imetelstat
Sorafenib + Imetelstat
B
Relative activity (%)
ALT
AST
AP
150
120
90
60
30
0
100
80
40
20
Vehicle
Sorafenib
Imetelstat
Sorafenib + Imetelstat
C
Relative hematocrit
20
10
0
-10
-20
Vehicle
Sorafenib
Imetelstat
Sorafenib + Imetelstat
D
Relative RBC count
20
10
0
-10
-20
Vehicle
Sorafenib
Imetelstat
Sorafenib + Imetelstat
E
Relative WBC count
20
10
0
-10
-20
Vehicle
Sorafenib
Imetelstat
Sorafenib + Imetelstat
F
Serum creatinine
Relative activity (%)
120
100
80
60
40
20
0
Vehicle
Sorafenib
Imetelstat
Sorafenib + Imetelstat

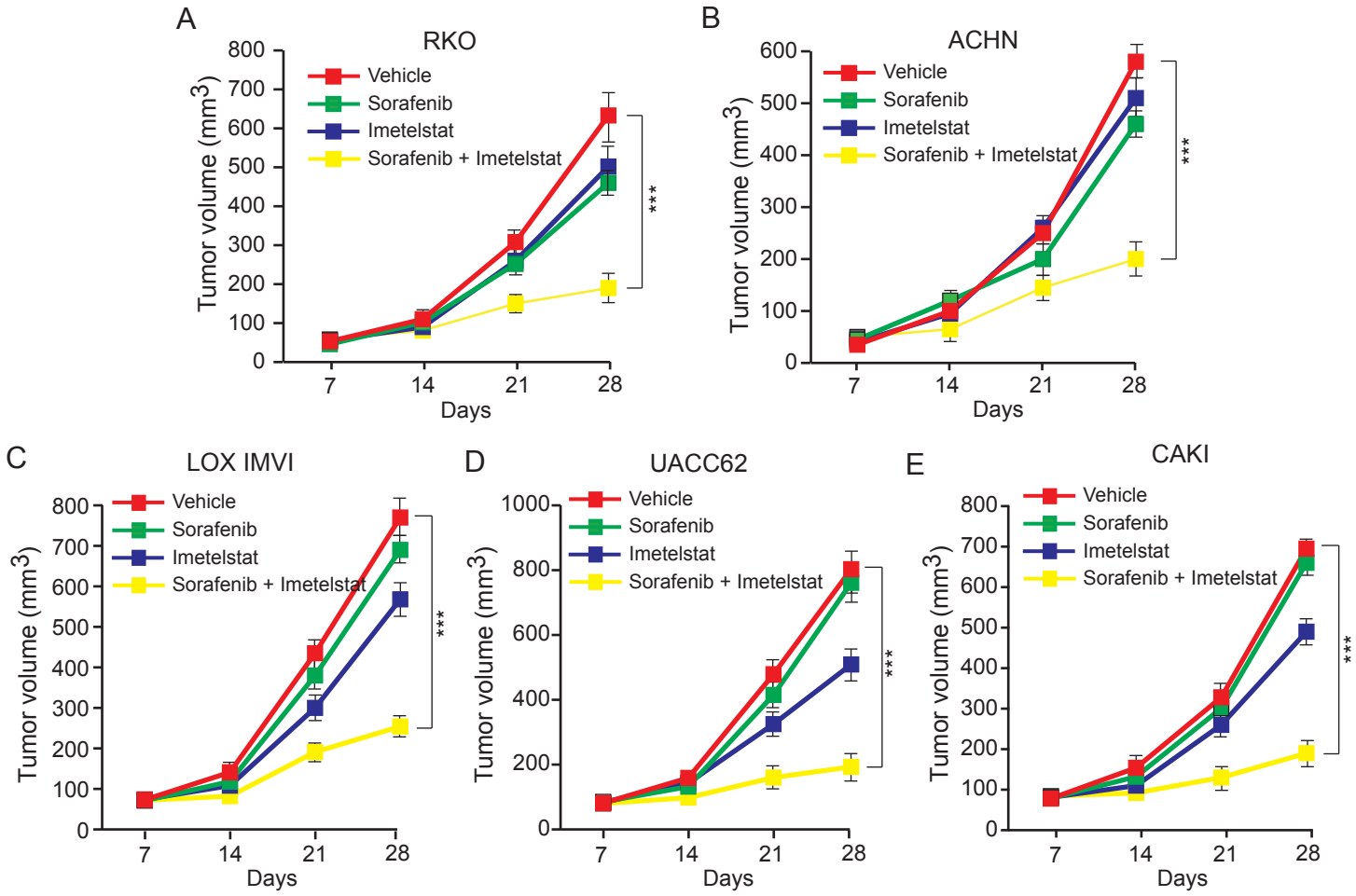
A
RKO
Vehicle
Sorafenib
Imetelstat
Sorafenib + Imetelstat
Tumor volume (mm3)
Days
***
B
ACHN
C
LOX IMVI
D
UACC62
E
CAKI

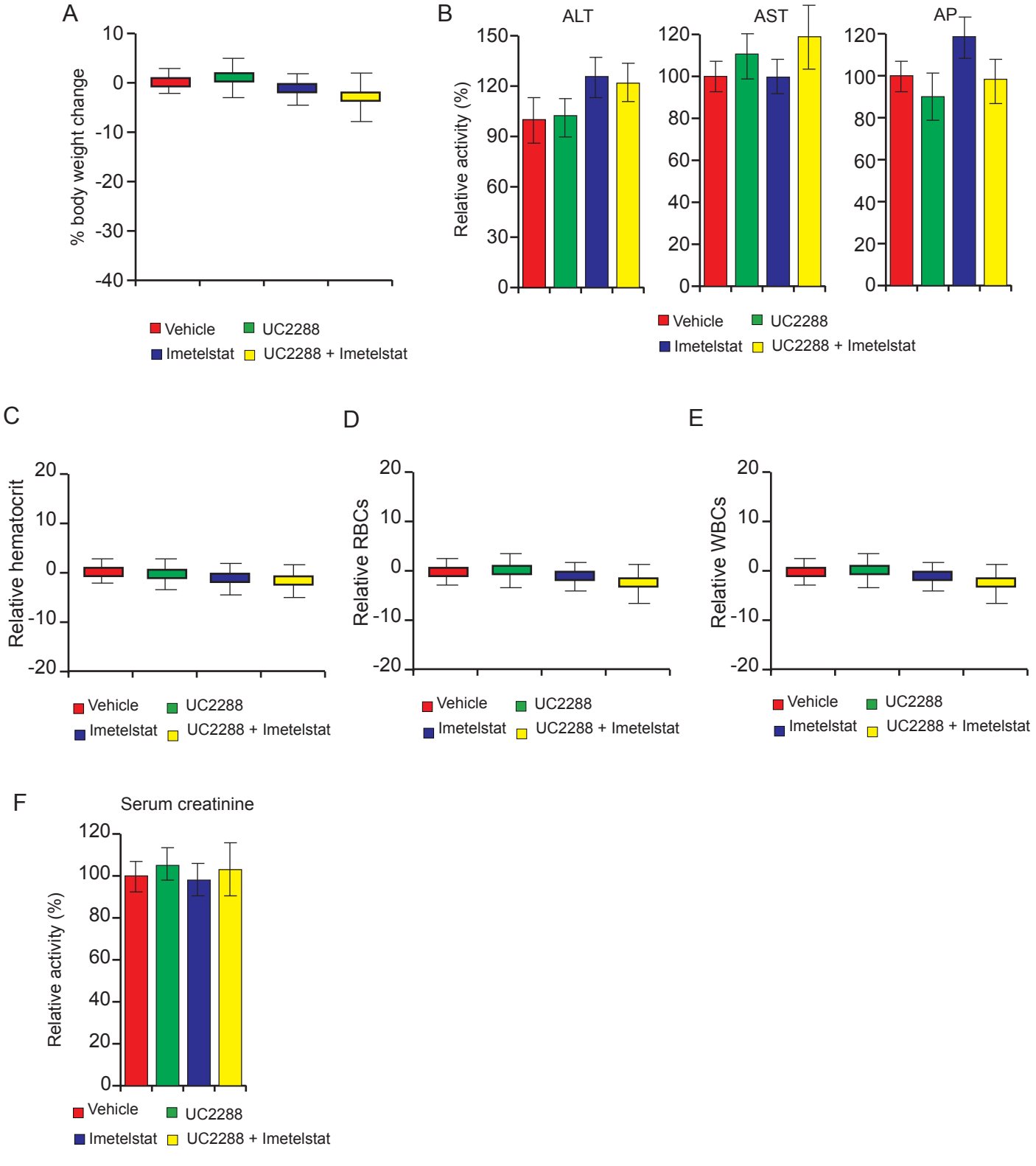
A
% body weight change
10
0
-10
-20
-30
-40
Vehicle
UC2288
Imetelstat
UC2288 + Imetelstat
B
ALT
AST
AP
Relative activity (%)
150
120
90
60
30
0
120
100
80
60
40
20
0
Vehicle
UC2288
Imetelstat
UC2288 + Imetelstat
C
Relative hematocrit
20
10
0
-10
-20
Vehicle
UC2288
Imetelstat
UC2288 + Imetelstat
D
Relative RBCs
20
10
0
-10
-20
Vehicle
UC2288
Imetelstat
UC2288 + Imetelstat
E
Relative WBCs
20
10
0
-10
-20
Vehicle
UC2288
Imetelstat
UC2288 + Imetelstat
F
Serum creatinine
Relative activity (%)
120
100
80
60
40
20
0
Vehicle
UC2288
Imetelstat
UC2288 + Imetelstat

Fig. S16

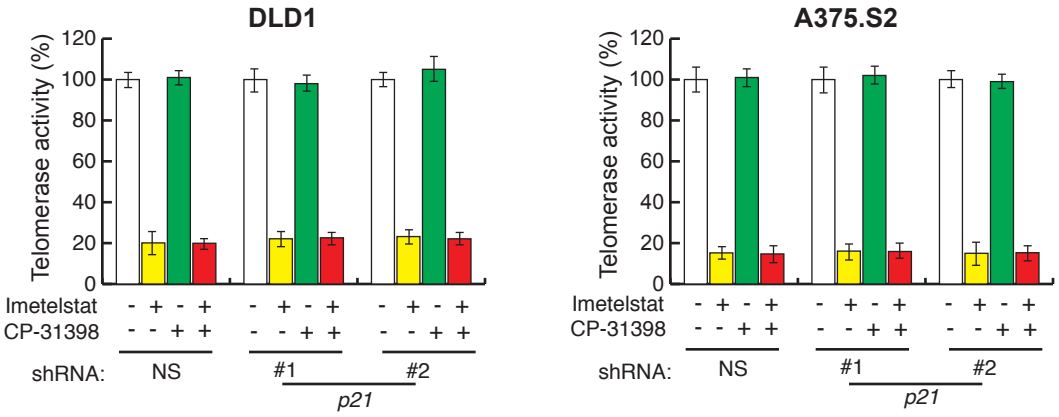
DLD1
A375.S2
Telomerase activity (%)
120
100
80
60
40
20
0
Imetelstat
CP-31398
shRNA:
NS
#1
#2
p21